Title

Semiautomated Characterization of Carotid Artery Plaque Features From Computed Tomography Angiography to Predict Atherosclerotic Cardiovascular Disease Risk Score.

Journal

Journal of Computer Assisted Tomography, 43(3)

ISSN

0363-8715

Authors

Zhu, Guangming
Li, Ying
Ding, Victoria
et al.

Publication Date

2019

DOI

10.1097/rct.0000000000000862

Peer reviewed

Published in final edited form as:

J Comput Assist Tomogr. 2019 ; 43(3): 452–459. doi:10.1097/RCT.0000000000000862.

Semiautomated Characterization of Carotid Artery Plaque Features From Computed Tomography Angiography to Predict Atherosclerotic Cardiovascular Disease Risk Score

Guangming Zhu, MD, PhD[*], **Ying Li, MD, PhD**[*,†], **Victoria Ding, MS**[‡], **Bin Jiang, MD, PhD**[*], **Robyn L. Ball, PhD**[‡], **Fatima Rodriguez, MD, MPH**[§], **Dominik Fleischmann, MD**[‖], **Manisha Desai, PhD**[‡], **David Saloner, PhD**[¶], **Ajay Gupta, MD, MS**[#], **Luca Saba, MD**[**], **Jason Hom, MD**[††], **Max Wintermark, MD, MAS**[*]

[*]Neuroradiology Section, Department of Radiology, Stanford University School of Medicine, Palo Alto, CA

[†]Department of Neurology, PLA Army General Hospital, Beijing, China

[‡]Department of Medicine, Quantitative Sciences Unit, Stanford University

[§]Division of Cardiovascular Medicine, Stanford University

[‖]Cardiovascular Imaging Section, Department of Radiology, Stanford University School of Medicine, Palo Alto

[¶]Department of Radiology, University of California San Francisco, San Francisco, CA

[#]Department of Radiology, Weill Cornell Medicine, New York, NY

[**]Dipartimento di Radiologia, Azienda Ospedaliero Universitaria di Cagliari, Italy.

[††]Department of Medicine, Stanford University School of Medicine, Palo Alto, CA

Abstract

Purpose: To investigate whether selected carotid computed tomography angiography (CTA) quantitative features can predict 10-year atherosclerotic cardiovascular disease (ASCVD) risk scores.

Methods: One hundred seventeen patients with calculated ASCVD risk scores were considered. A semiautomated imaging analysis software was used to segment and quantify plaque features. Eighty patients were randomly selected to build models using 14 imaging variables and the calculated ASCVD risk score as the end point (continuous and binarized). The remaining 37 patients were used as the test set to generate predicted ASCVD scores. The predicted and observed ASCVD risk scores were compared to assess properties of the predictive model.

Results: Nine of 14 CTA imaging variables were included in a model that considered the plaque features in a continuous fashion (model 1) and 6 in a model that considered the plaque features

Correspondence to: Max Wintermark, MD, MAS, Neuroradiology Section, Department of Radiology, Stanford University School of Medicine, 300 Pasteur Dr, Grant S047, Stanford, CA 94305 (max.wintermark@gmail.com).
J.H. and M.W. are co-senior authors.

The authors declare no conflict of interest.

dichotomized (model 2). The predicted ASCVD risk scores were 18.87% ± 13.26% and 18.39% ± 11.6%, respectively. There were strong correlations between the observed ASCVD and the predicted ASCVDs, with $r = 0.736$ for model 1 and $r = 0.657$ for model 2. The mean biases between observed ASCVD and predicted ASCVDs were −1.954% ± 10.88% and −1.466% ± 12.04%, respectively.

Conclusions: Selected quantitative imaging carotid features extracted from the semiautomated carotid artery analysis can predict the ASCVD risk scores.

Keywords

ASCVD; carotid plaque; computed tomography angiography; semiautomatic

Atherosclerotic plaques may develop in the carotid arteries, with clinical sequelae of cerebrovascular disease.[1] Accurate quantification of carotid plaque features is important as a complement to luminal stenosis measurements, because these features have been reported as being associated with an increased risk of stroke and cardiovascular disease.[2–7]

Carotid artery atherosclerotic plaques can be assessed using several different imaging modalities.[8,9] Routinely acquired computed tomography angiography (CTA) holds significant potential in identifying high-risk plaque features.[10] Computed tomography angiography allows for a fast and reliable evaluation of the carotid arteries and is able to assess both carotid lumen and carotid plaques, including plaque surface morphology and plaque composition.[11,12] Using CTA to characterize carotid plaque volume and composition has been validated both in ex vivo and in vivo studies, using histology as the criterion standard.[13–15]

In 2013, the American College of Cardiology and the American Heart Association released new recommendations using the 10-year atherosclerotic cardiovascular disease (ASCVD) risk scores to guide initiation of statin treatment for patients with high risk of ischemic vascular diseases.[16] Previous studies suggest some associations, but not a perfect overlap between ASCVD risk score and the carotid artery imaging findings extracted from CTA.[17] A substantial fraction of patients with high 10-year ASCVD risk scores have minimal imaging abnormalities, and a significant fraction of patients with low 10-year ASCVD risk scores have imaging abnormalities. Carotid artery imaging can be more precise and provide improved prognostic information, allowing for better decision-making strategies.

However, visual assessment of carotid artery imaging is subjective and influenced by the experience of the reviewer.[18] In addition, manual measurements of variables such as the degree of carotid artery stenosis or the maximal carotid plaque thickness are time consuming and prone to interoperator and intraoperator variability.[14] Semiautomated approachesto assess CTA carotid artery imaging can extract multiple anatomic and compositional features rapidly and quantitatively.[19,20] These features may be used to predict stroke and cardiovascular events and may have advantages over the ASCVD risk score.

Our goals in this study were to determine whether selected quantitative features from a semiautomated analysis of carotid CTA can be used to predict the ASCVD risk scores and

whether there are appropriate cutoff values for these quantitative features to predict the ASCVD risk scores.

MATERIALS AND METHODS

Study Population

We retrospectively identified a series of patients who underwent a head and neck CTA at our institution from January 2014 to July 2016. This study was approved by our institutional internal review board. Our institutional review board waived patient consent because of its retrospective nature. Clinical information was gathered from our electronic medical record to calculate the 10-year ASCVD scores using the Pooled Cohort Equations from the 2013 American College of Cardiology and the American Heart Association guidelines.[16] Patients who met one or more of the following conditions were excluded: (1) age outside the 40- to 79-year range; (2) total cholesterol outside the 130- to 320-mg/dL range; (3) high-density lipoprotein (HDL) cholesterol outside the 20- to 100-mg/dL range; (4) systolic blood pressure outside the 90- to 200-mm Hg range; (5) no smoking status record; (6) received a coronary artery bypass graft or a carotid endarterectomy; (7) more than 6 months elapsed between the clinical visit/blood draw to measure the clinical variables and the imaging study; (8) poor quality of CTA owing to motion artifacts or other issues that interfered with postprocessing. A flowchart outlining patient selection is shown in Figure 1.

Carotid Artery CTA Acquisition Protocol

The CTA studies of the carotid arteries were performed on 16- or 64-slice computed tomography scanners (GE Healthcare, Milwaukee, Illinois) and (Siemens Healthcare, Erlangen, Germany) in helical mode. The carotid artery CTA, covering the midchest to the vertex of the brain, was collimated at 1 to 1.25 mm using 120 kVp and 240 mAs, and a rotation time of 0.6 to 0.8 second. A bolus of 70 to 80 mL of Isovue 300 or 370 (lopamidol; Bracco Diagnostics Inc, Monroe Township, NJ) was injected into an antecubital vein with a power injector at a rate of 4 to 5 mL/s. SmartPrep protocol was applied to monitor the contrast enhancement and trigger the CTA acquisition. Effective dose associated with the carotid artery CTA protocol was 5 to 7 mSv.

Imaging Review

Common carotid arteries and the cervical portion of the internal carotid arteries were assessed using a commercially available, semiautomated software package for atherosclerotic plaque imaging analysis (vascuCAP; Elucid Bioimaging, Wenham, Mass).[21,22] The common carotid artery and the cervical portion of the internal carotid artery were defined, and the software package automatically calculated a centerline, as well as lumen and wall segmentations.[22] Within the segmentations, the software package then quantified features such as luminal diameter and wall thickness and tissue characteristics (Fig. 2). A total of 32 plaque features for each patient were thus calculated, and 14 of them were selected as imaging variables for further analysis (Table 1), as these were previously demonstrated as the most clinically relevant by Gupta et al.[21]

Statistical Analysis

Training and Test Sets—Of all 117 cases, 80 cases were randomly selected using "sample" functions in R and then used as a training set to develop a classification model. The remaining 37 cases comprised the test set and were used to evaluate the predictive ability of the classification model.

Descriptive Statistics—We compared the demographic and imaging variables between 2 groups of patients. We used Mann-Whitney U tests for continuous variables (age, total cholesterol, HDL cholesterol, systolic blood pressure, 10-year ASCVD score, and 14 selected imaging variables generated by vascuCAP) and χ^2 tests for binary variables (sex, arterial hypertension, diabetes history, and smoking history).

Multivariable Linear Regression Models—Generalized linear regression techniques were used to develop classification models. Using the training set, we performed multiple linear regression analyses using lm steps with backward in RStudio Desktop (Mac OS version 1.1.456, Boston, Mass). The calculated 10-year ASCVD risk was set as dependent variable. In model 1, the 14 imaging variables from vascuCAP were included as predictor variables. We also defined cutoff values for all those 14 imaging variables from vascuCAP to facilitate the clinical use of the software results. Histograms of those variables were used to determine cutoff values visually and to dichotomize these variables (Fig. 3). In model 2, these 14 binary variables were included as predictor variables.

With the test set, we used models 1 and 2 to generate predicted ASCVDs. One-way analyses of variance were used to analyze the differences among and the observed ASCVD and 2 ASCVDs predicted by models 1 and 2. Correlations between the observed ASCVD and the ASCVD predicted by model 1 or 2 were calculated using Pearson correlation tests. Bland-Altman analyses were used to assess the biases within 3 ASCVDs, respectively.

All statistical analyses were conducted using RStudio Desktop (Mac OS version 1.1.456). Statistical significance was set at $\alpha < 0.05$.

RESULTS

Among 1405 patients who underwent carotid artery CTA during the study period, 117 patients met the inclusion criteria and were included in the study cohort. These included 56 females and 61 males with a mean age of 61.62 ± 10.01 years (range, 40–79 years). Mean ASCVD risk was 16.06% ± 14.66%. There were no significant demographic differences between the training and test sets (Table 2). Three imaging variables showed significant differences between the training and test sets (Table 2): vessel volume that includes the lumen and wall ($P < 0.001$), maximum calcified area proportion ($P = 0.001$), and wall volume divided by vessel volume inclusive of lumen and wall ($P < 0.001$).

Cutoff values of imaging variables were generated visually according to the histograms describing the distribution of their values (Fig. 3). There were 9 variables included in model 1 and 6 variables included in model 2 (Table 3).

In the test set, the observed ASCVD was 16.92% ± 15.90%. The ASCVD predicted by model 1 (semiautomated approach, continuous imaging features) was 18.87% ± 13.26% and 18.39 (± 11.6% by model 2 (semiautomated approach, dichotomized imaging features). There were no significant differences among 3 ASCVDs ($P = 0.424$, Fig. 4A).

There were good correlations between the observed ASCVD and the ASCVD predicted by model 1 ($r = 0.736$; 95% CI, 0.540–0.856) and between the observed ASCVD and the ASCVD predicted by model 2 ($r = 0.657$; 95% CI, 0.423–0.809). Predicted ASCVDs by models 1 and 2 had an excellent correlation with each other ($r = 0.900$; 95% CI, 0.807–0.946).

The mean value bias between observed ASCVD and predicted ASCVD according to model 1 was −1.954% ± 10.88%. It was −1.466% ± 12.04% between observed ASCVD and predicted ASCVD according to model 2. It was 0.488% ± 5.88% between the 2 models (Table 4 and Figs. 4B–D).

DISCUSSION

In this study, we used selected multiple quantitative features from a semiautomated analysis to generate statistical models to predict the ASCVD risk scores. Our results suggest that a CTA-based, semiautomated plaque analysis can provide a quantitative technique in identifying patients at high risk of stroke/cardiovascular events. Nine carotid imaging features with continuous values and 6 carotid imaging features with dichotomized values were included in the models. Both models included the same 3 features: maximum lipid-rich necrotic core area, thickest wall across all cross sections of the target, and maximum cross-sectional wall area, which had a significant positive correlation with the 10-year ASCVD risk scores. Maximum cross-sectional dilation based on lumen diameter had significant negative correlation with the 10-year ASCVD risk scores. Interestingly, the presence of calcium in the plaques was not retained in any of the models, confirming previous findings that calcium in the carotid artery plaque should not be considered a risk factor.[23] Several studies have also demonstrated the stabilizing role of calcium not only in carotid artery studies, but also in coronary artery studies.[24–26]

The degree of stenosis or luminal narrowing is the accepted, primary diagnostic criterion used to evaluate the severity of carotid atherosclerosis.[27] Many studies and trials suggest that significant arterial stenosis (70%–99%) is a reliable marker to identify those patients at highest risk of future ischemic stroke.[28,29] However, because of the existence of positive remodeling, the presence of a large atherosclerotic plaque is not always associated with luminal narrowing.[30] In addition, studies on carotid plaque also suggest plaque morphology, and composition can be used to predict the risk of future ischemic events.[31,32] Recent studies have suggested that routine CTA can be used to assess the high-risk features of carotid artery plaques, because CTA provides tissue attenuation data that allows the identification of different plaque components[10,33,34] in the vessel wall.

The ASCVD risk score, which quantifies the risk of stroke and cardiovascular events, can be calculated from age, sex, race, blood pressure, cholesterol values, diabetes mellitus, and

smoking status. Previous studies demonstrated that patients with high 10-yearASCVD risk scores have more advanced CTA imaging features of carotid artery atherosclerosis.[17] However, in those studies, plaque imaging analysis on CTA was performed by subjective review by imaging experts, which suffers from limited intraobserver and interobserver reproducibility.

Accurate quantification of specific plaque features, such as anatomic structure and tissue characteristics, based on a semiautomated approach, can be more reliable and less time consuming. Several studies validated that a semiautomatic CTA-based image segmentation approach, using an imaging processing software package benchmarked against histopathologic examinations of endarterectomy specimens, can identify, locate, characterize, and quantify atherosclerotic plaques in carotid artery.[19–21,35–40] However, whether selected quantitative features from the semiautomated approach can be used to predict the ASCVD risk scores has not previously been determined.

Our study was limited in that it was a retrospective study in a single center with limited power. Although 10-year ASCVD risk score has been widely used, it is only a surrogate end point, not the criterion standard to predict stroke and cardiovascular disease. Further studies are needed to validate our results and also to prospectively determine the real correlations between plaque imaging features and future stroke/cardiovascular events as could be determined in a prospective study. Another limitation is that carotid CTA is unlikely to be used routinely for risk prediction for primary prevention. However, an important point is that CTA plaque characterization is useful in ASCVD risk prediction, beyond just plaque stenosis, especially for patients at higher risk.

In conclusion, our study determined that selected quantitative imaging carotid features extracted from the semiautomated analysis of the carotid arteries can be used to predict the observed ASCVD risk scores.

ACKNOWLEDGMENTS

The authors thank Elucid Bioimaging for providing the atherosclerotic plaque imaging analysis software (vascuCAP) at no cost for the authors to implement in their study. Elucid Bioimaging was not involved in the design, analysis, or any other aspect of the study.

REFERENCES

1. Evans NR, Tarkin JM, Chowdhury MM, et al. PET imaging of atherosclerotic disease: advancing plaque assessment from anatomy to pathophysiology. Curr Atheroscler Rep. 2016;18:30. [PubMed: 27108163]
2. Rothwell PM, Gibson R, Warlow CP. Interrelation between plaque surface morphology and degree of stenosis on carotid angiograms and the risk of ischemic stroke in patients with symptomatic carotid stenosis. Stroke. 2000; 31:615–621. [PubMed: 10700494]
3. Lorenz MW, von Kegler S, Steinmetz H, et al. Carotid intima-media thickening indicates a higher vascular risk across a wide age range: prospective data from the Carotid Atherosclerosis Progression Study (CAPS). Stroke. 2006;37:87–92. [PubMed: 16339465]
4. Takaya N, Yuan C, Chu B, et al. Association between carotid plaque characteristics and subsequent ischemic cerebrovascular events: a prospective assessment with MRI—initial results. Stroke. 2006;37:818–823. [PubMed: 16469957]

5. Van den Oord SC, Sijbrands EJ, Gerrit L, et al. Carotid intima-media thickness for cardiovascular risk assessment: systematic review and meta-analysis. Atherosclerosis. 2013;228:1–11. [PubMed: 23395523]
6. Jashari F, Ibrahimi P, Bajraktari G, et al. Carotid plaque echogenicity predicts cerebrovascular symptoms: a systematic review and meta-analysis. Eur J Neurol. 2016;23:1241–1247. [PubMed: 27106563]
7. Saam T, Hetterich H, Hoffmann V, et al. Meta-analysis and systematic review of the predictive value of carotid plaque hemorrhage on cerebrovascular events by magnetic resonance imaging. JAmColl Cardiol. 2013;62:1081–1091.
8. Vancraeynest D, Pasquet A, Roelants V, et al. Imaging the vulnerable plaque. J Am Coll Cardiol. 2011;57:1961–1979. [PubMed: 21565634]
9. Spacek M, Zemanek D, Hutyra M, et al. Vulnerable atherosclerotic plaque—a review of current concepts and advanced imaging. Biomed Pap. 2018;162:10–17.
10. Bartlett ES, Walters TD, Symons SP, et al. Quantification of carotid stenosis on CT angiography. Am J Neuroradiol. 2006;27:13–19. [PubMed: 16418349]
11. Van Gils MJ. Insight Into Carotid Atherosclerotic Plaque Development With CT Angiography. Erasmus University Rotterdam: Rotterdam, The Netherlands; 2017.
12. Das M, Braunschweig T, Muhlenbruch G, et al. Carotid plaque analysis: comparison of dual-source computed tomography (CT) findings and histopathological correlation. Eur J Vasc Endovasc Surg. 2009;38: 14–19. [PubMed: 19464932]
13. de Weert TT, Ouhlous M, Meijering E, et al. In vivo characterization and quantification of atherosclerotic carotid plaque components with multidetector computed tomography and histopathological correlation. Arterioscler Thromb Vasc Biol. 2006;26:2366–2372. [PubMed: 16902158]
14. de Weert TT, de Monye C, Meijering E, et al. Assessment of atherosclerotic carotid plaque volume with multidetector computed tomography angiography. Int J Cardiovasc Imaging. 2008;24:751–759. [PubMed: 18373211]
15. Wintermark M, Jawadi SS, Rapp JH, et al. High-resolution CT imaging of carotid artery atherosclerotic plaques. AJNR Am J Neuroradiol. 2008;29: 875–882. [PubMed: 18272562]
16. Goff DC, Lloyd-Jones DM, Bennett G, et al. 2013 ACC/AHA guideline on the assessment of cardiovascular risk: a report of the American College of Cardiology/American Heart Association Task Force on Practice Guidelines. J Am Coll Cardiol. 2014;63:2935–2959. [PubMed: 24239921]
17. Li Y, Zhu G, Ding V, et al. Assessing the relationship between American Heart Association atherosclerotic cardiovascular disease risk score and carotid artery imaging findings. J of Computer Assisted Tomography Accepted.
18. Vukadinovic D, Rozie S, van Gils M, et al. Automated versus manual segmentation of atherosclerotic carotid plaque volume and components in CTA: associations with cardiovascular risk factors. Int J Cardiovasc Imaging. 2012;28:887–887.
19. Hemmati HR, Alizadeh M, Kamali-Asl A, et al. Semi-automated carotid lumen segmentation in computed tomography angiography images [published online ahead of print November 5, 2017]. J Biomed Res. 2017.
20. Saba L, Gao H, Acharya UR, et al. Analysis of carotid artery plaque and wall boundaries on CT images by using a semi-automatic method based on level set model. Neuroradiology. 2012;54:1207–1214. [PubMed: 22562690]
21. Gupta A, Al-Dasuqi K, Hooman K, et al. Semi-automated detection of high-risk atherosclerotic carotid artery plaque features from computed tomography angiography. Berlin, Germany: Presented at the European Stroke Conference; 2017.
22. Sheahan M, Ma X, Paik D, et al. Atherosclerotic plaque tissue: noninvasive quantitative assessment of characteristics with software-aided measurements from conventional CT angiography. Radiology. 2017;286: 622–631. [PubMed: 28858564]
23. Nandalur KR, Hardie AD, Raghavan P, et al. Composition of the stable carotid plaque: insights from a multidetector computed tomography study of plaque volume. Stroke. 2007;38:935–940. [PubMed: 17272781]

24. Hunt JL, Fairman R, Mitchell ME, et al. Bone formation in carotid plaques: a clinicopathological study. Stroke. 2002;33:1214–1219. [PubMed: 11988593]
25. Shaalan WE, Cheng H, Gewertz B, et al. Degree of carotid plaque calcification in relation to symptomatic outcome and plaque inflammation. J Vasc Surg. 2004;40:262–269. [PubMed: 15297819]
26. Beckman JA, Ganz J, Creager MA, et al. Relationship of clinical presentation and calcification of culprit coronary artery stenoses. Arterioscler Thromb Vasc Biol. 2001;21:1618–1622. [PubMed: 11597935]
27. Barnett HJ, Taylor DW, Eliasziw M, et al. Benefit of carotid endarterectomy in patients with symptomatic moderate or severe stenosis. North American Symptomatic Carotid Endarterectomy Trial Collaborators. N Engl J Med. 1998;339:1415–1425. [PubMed: 9811916]
28. Ederle J, Dobson J, Featherstone RL, et al. Carotid artery stenting compared with endarterectomy in patients with symptomatic carotid stenosis (International Carotid Stenting Study): an interim analysis of a randomised controlled trial. Lancet. 2010;375:985–997. [PubMed: 20189239]
29. Meier P, Knapp G, Tamhane U, et al. Short term and intermediate term comparison of endarterectomy versus stenting for carotid artery stenosis: systematic review and meta-analysis of randomised controlled clinical trials. BMJ. 2010;340:c467. [PubMed: 20154049]
30. Underhill HR, Yuan C, Yarnykh VL, et al. Arterial remodeling in [corrected] subclinical carotid artery disease. JACC Cardiovasc Imaging. 2009;2:1381–1389. [PubMed: 20083072]
31. Ibrahimi P, Jashari F, Nicoll R, et al. Coronary and carotid atherosclerosis: how useful is the imaging? Atherosclerosis. 2013;231: 323–333. [PubMed: 24267246]
32. DeMarco JK, Huston J 3rd. Imaging of high-risk carotid artery plaques: current status and future directions. Neurosurg Focus. 2014;36:E1.
33. Gupta A, Mtui EE, Baradaran H, et al. CT angiographic features of symptom-producing plaque in moderate-grade carotid artery stenosis. AmJ Neuroradiol. 2014.
34. Gupta A, Baradaran H, Kamel H, et al. Evaluation of computed tomography angiography plaque thickness measurements in high-grade carotid artery stenosis. Stroke. 2014;45:740–745. [PubMed: 24496392]
35. Bleeker L, Marquering HA, van den Berg R, et al. Semi-automatic quantitative measurements of intracranial internal carotid artery stenosis and calcification using CT angiography. Neuroradiology. 2012;54:919–927. [PubMed: 22205339]
36. dos Santos FL, Joutsen A, Terada M, et al. A semi-automatic segmentation method for the structural analysis of carotid atherosclerotic plaques by computed tomography angiography. J Atheroscler Thromb. 2014;21: 930–940. [PubMed: 24834981]
37. Wintermark M, Glastonbury C, Tong E, et al. Semi-automated computer assessment of the degree of carotid artery stenosis compares favorably to visual evaluation. J Neurol Sci. 2008;269:74–79. [PubMed: 18234230]
38. Hemmati H, Kamli-Asl A, Talebpour A, et al. Semi-automatic 3D segmentation of carotid lumen in contrast-enhanced computed tomography angiography images. Phys Med. 2015;31:1098–1104. [PubMed: 26429385]
39. Scherl H, Hornegger J, Prummer M, et al. Semi-automatic level-set based segmentation and stenosis quantification of the internal carotid artery in 3D CTA data sets. Med Image Anal. 2007;11:21–34. [PubMed: 17126064]
40. Saba L, Sanfilippo R, Montisci R, et al. Carotid artery stenosis quantification: concordance analysis between radiologist and semi-automatic computer software by using multi-detector-row CT angiography. Eur J Radiol. 2011;79:80–84. [PubMed: 20031358]

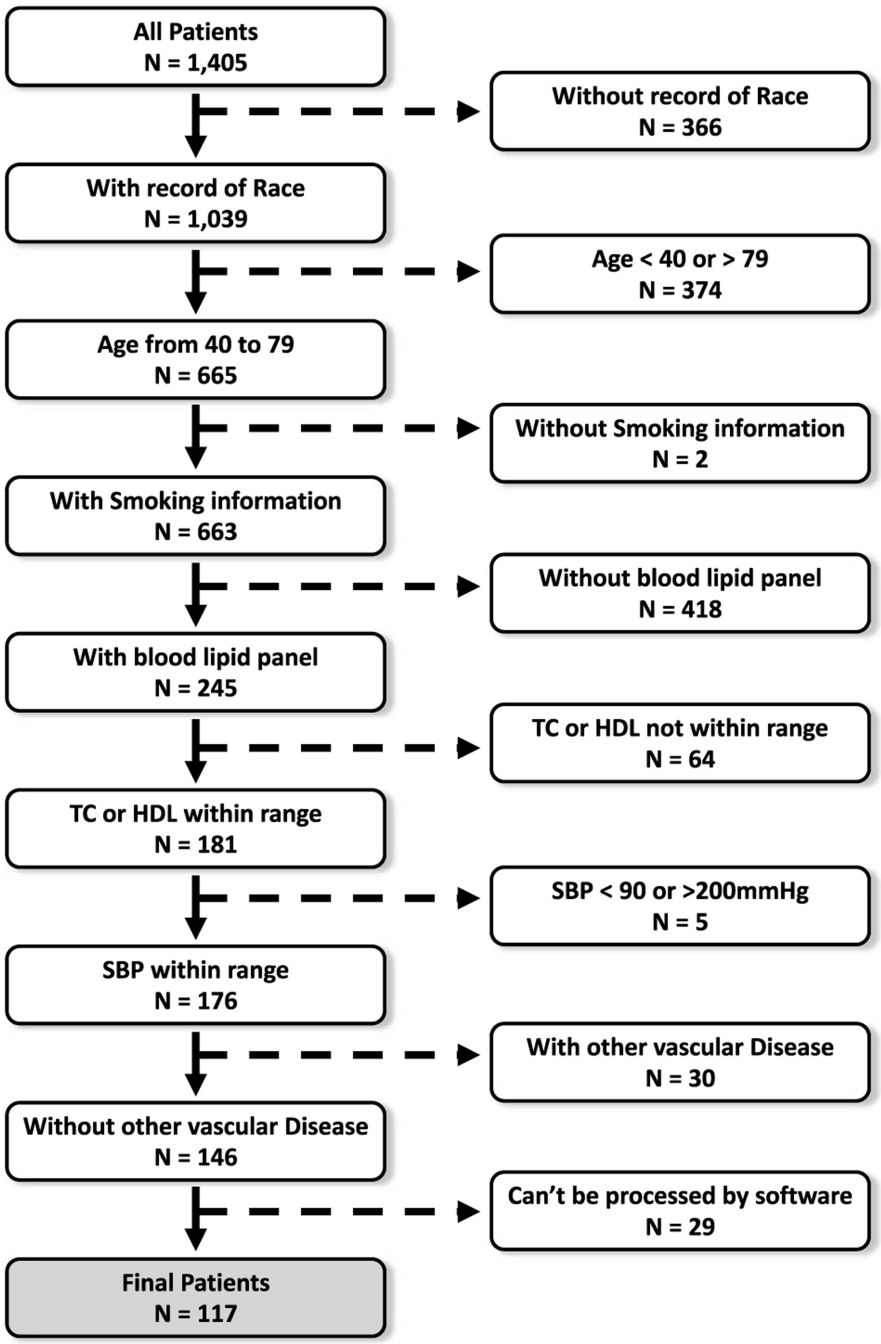

FIGURE 1.
Flowchart outlining patient selection.

FIGURE 2.

Example of segmentation and analysis of common and internal carotid arteries. Up, The 3-dimensional segmentation of lumen and vessel wall of common and internal carotid arteries and their cross-sectional representations of lumen and wall. Down, The analysis of plaque components (yellow = LRNC, blue = matrix, green = calcification, red = intraplaque hemorrhage if it exists) of left carotid artery in axial, coronal, and sagittal planes.

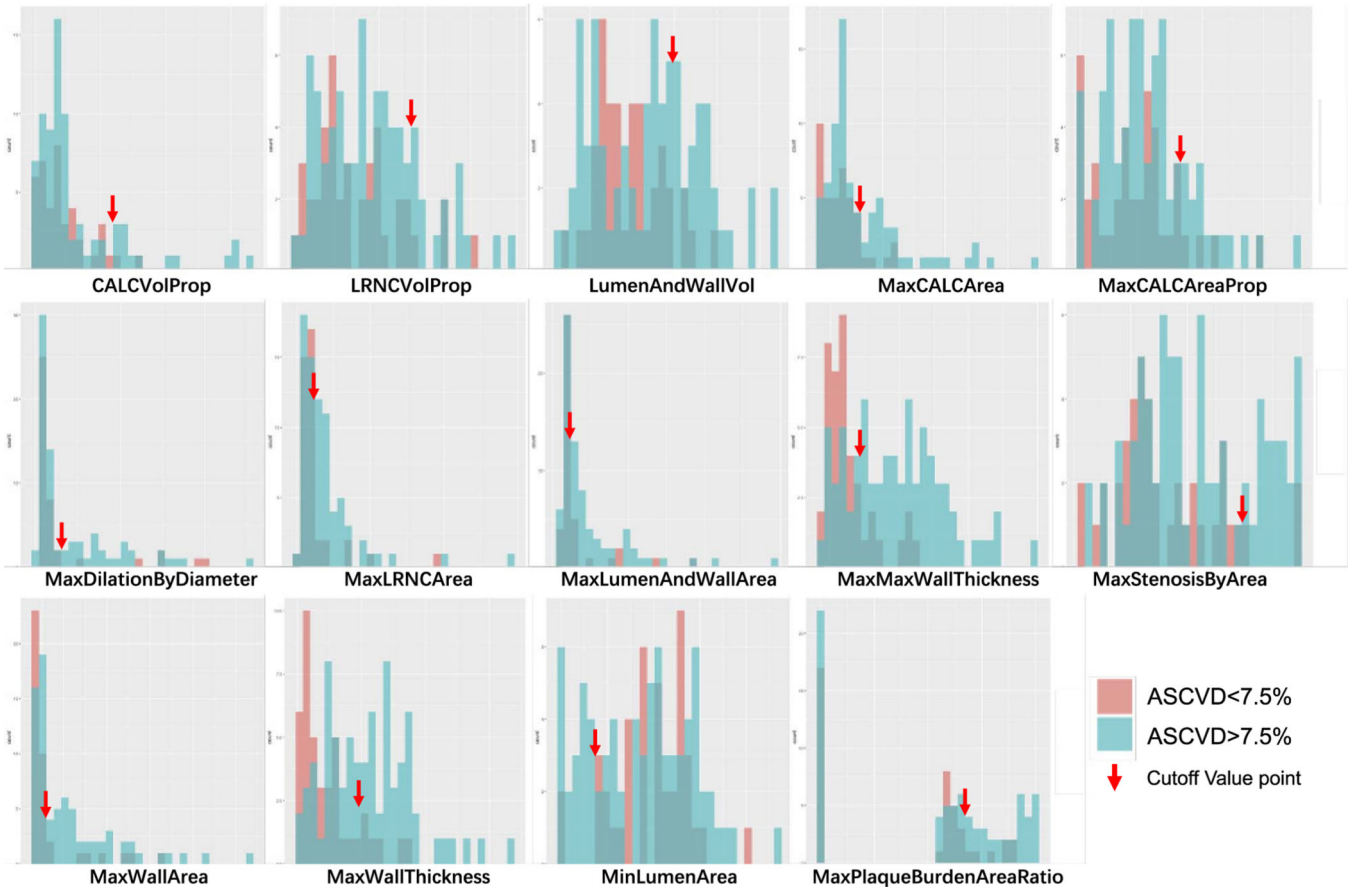

FIGURE 3.

Histogram for 14 carotid artery features on CTA and the corresponding cutoff values (arrows).

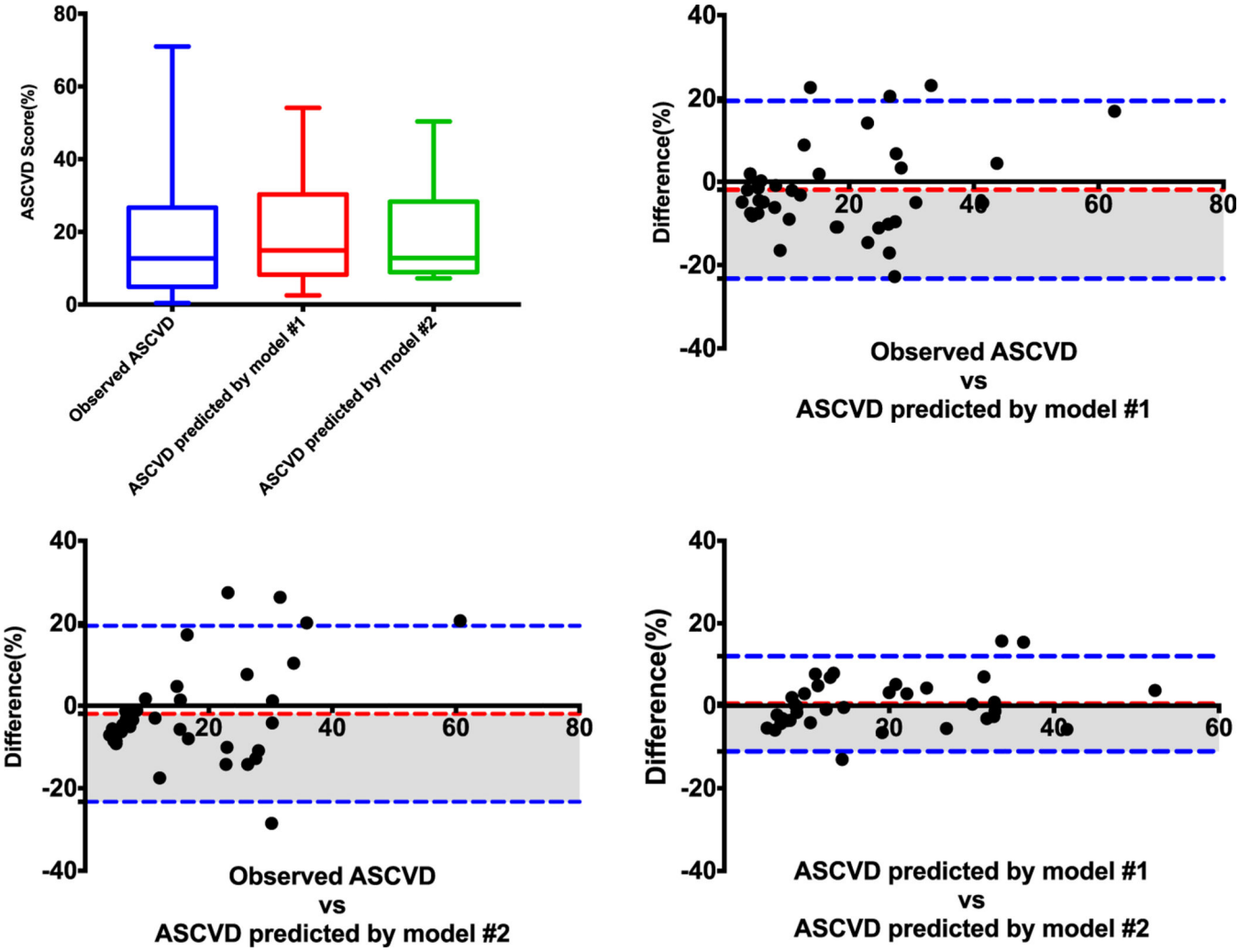

FIGURE 4.

Differences among observed ASCVD and ASCVD predicted by model 1 (semiautomated approach, continuous imaging features) and model 2 (semiautomated approach, dichotomized imaging features).

TABLE 1.

List of Carotid Artery Imaging Features Extracted Semiautomatically by the Processing Package and Cutoff Values Used to Dichotomize Them

Carotid Artery Imaging Features	Cutoff Value
Vessel volume that includes the lumen and wall	2200 mm^3
Maximal cross-sectional lumen and vessel wall area	900 mm^2
Minimal cross-sectional lumen area	1.5 mm^2
Maximal cross-sectional stenosis based on area	75%
Minimal cross-sectional lumen diameter	3%
Wall volume divided by vessel volume inclusive of lumen and wall.	65%
Maximal cross-sectional wall area	70mm^2
Thickest wall assessed 3-dimensionally when indicated at the target or vessel level	4.5 mm
Thickest wall across all cross sections of the target	4.5 mm
Lipid rich necrotic core volume as a proportion of total wall volume	0.14
Maximal lipid-rich necrotic core area	95 mm^2
Calcified volume as a proportion of total wall volume	0.1
Maximal calcified area proportion	0.55
Maximal cross-sectional calcified area	28 mm^2

J Comput Assist Tomogr. Author manuscript; available in PMC 2021 April 28.

J Comput Assist Tomogr. Author manuscript; available in PMC 2021 April 28.

TABLE 2.

Basic Demographic Information and Imaging Variables Values by vascuCAP

	Overall (n = 117)	Development Patient Set (n = 80)	Validation Patient Set (n = 37)	*P*
Demographic information				
Female sex, n (%)	56 (47.9%)	40 (50.0)	16 (43.2)	0.463
Age, mean ± SD, y	61.62 ± 10.01	62.54 ± 9.57	59.62 ± 10.76	0.342
Active smoker, n (%)	14 (11.97)	7 (8.75)	7 (18.92)	0.289
History of smoking, n (%)	13 (11.11)	7 (8.75)	6 (16.22)	0.490
Smoking, mean ± SD, packs/y	23.65 ± 31.53	23.56 ± 34.8	23.84 ± 24.47	1.000
Systolic blood pressure, mean ± SD, mm Hg	134.5 ± 20.2	132.90 ± 19.40	137.80 ± 21.20	0.477
Antihypertension medication, n (%)	65 (55.56)	41 (51.25)	24 (64.86)	0.387
Total cholesterol, mean ± SD, mg/dL	183.70 ± 35.73	183.10 ± 36.15	185.10 ± 35.25	0.962
HDL, mean ± SD, mg/dL	49.98 ± 15.15	50.66 ± 15.38	48.51 ± 14.75	0.776
Cholesterol-lowering medication, n (%)	70 (59.83)	53 (66.25)	17 (45.95)	0.114
History of diabetes, n (%)	35 (29.91)	21 (26.25)	14 (37.84)	0.445
Hemoglobin A_{1c}, mean ± SD, %	7.20 ± 2.12	6.88 ± 2.05	8.21 ± 2.14	0.299
Diabetes treatment, n (%)	29 (24.79)	17 (21.25)	12 (32.43)	0.428
ASCVD score, %	16.06 ± 14.66	15.66 ± 14.14	16.92 ± 15.90	0.668
NASCET, %	6.18 ± 15.07	4.33 ± 13.95	7.04 ± 15.56	0.652
Imaging variables				
Calcified volume as a proportion of total wall volume.	0.028 ± 0.032	0.024 ± 0.029	0.036 ± 0.037	0.175
LRNC volume as a proportion of total wall volume	0.086 ± 0.051	0.087 ± 0.048	0.084 ± 0.057	0.062
Vessel volume that includes the lumen and wall, mm^3	16.25 ± 5.61	18.13 ± 5.17	12.19 ± 4.22	<0.001
Maximum cross-sectional calcified area, mm^2	14.53 ± 15.55	12.47 ± 16.52	18.98 ± 12.24	0.107
Maximum calcified area proportion	0.257 ± 0.176	0.217 ± 0.172	0.345 ± 0.151	0.001
Maximum cross-sectional dilation based on lumen diameter, %	3.838 ± 5.108	4.041 ± 5.534	3.400 ± 4.072	0.820
Maximum lipid-rich necrotic core area, mm^2	17.44 ± 20.12	17.40 ± 17.12	17.52 ± 25.72	1.000
Maximum cross-sectional lumen and vessel wall area, mm^2	208.4 ± 227.0	218.4 ± 253.7	186.7 ± 155.1	0.783
Thickest wall across all cross sections of the target, mm	3.414 ± 1.360	3.319 ± 1.272	3.620 ± 1.532	0.538
Maximum cross-sectional stenosis based on area, %	49.69 ± 26.44	49.10 ± 23.00	50.98 ± 33.01	0.938
Maximum cross-sectional wall area, mm^2	97.43 ± 93.10	96.84 ± 94.13	98.70 ± 92.12	0.995

	Overall (n = 117)	Development Patient Set (n = 80)	Validation Patient Set (n = 37)	*P*
Thickest wall assessed 3-dimensionally when indicated at the target or vessel level, mm	3.764 ± 1.354	3.717 ± 1.205	3.868 ± 1.643	0.854
Minimum cross-sectional lumen area, mm^2	8.952 ± 5.084	9.528 ± 4.809	7.708 ± 5.497	0.197
Wall volume divided by vessel volume inclusive of lumen and wall, %	49.29 ± 37.11	36.26 ± 36.86	77.46 ± 16.19	<0.001

LRNC indicates lipid rich necrotic core; NASCET, North American Symptomatic Carotid Endarterectomy Trial.

J Comput Assist Tomogr. Author manuscript; available in PMC 2021 April 28.

TABLE 3.

Linear Regression Analysis for Model 1 (Semiautomated Approach, Continuous Imaging Features) and Model 2 (Semiautomated Approach, Dichotomized Imaging Features)

	Model 1 (Semiautomated Approach, Continuous Imaging Features)						Model 2 (Semiautomated Approach, Dichotomized Imaging Features)					
		95% CI						95% CI				
Maximum Lipid	**Estimate**	**Lower**	**Upper**	**SE**	***t***	***P***	**Estimate**	**Lower**	**Upper**	**SE**	***t***	***P***
(Intercept)	−12.04	−25.320	1.239	6.658	−1.808	0.075	4.966	0.936	8.995	2.021	2.456	0.016
LRNC volume as a proportion of total wall volume	52.16	−25.670	129.985	39.02	1.337	0.186	—	—	—	—	—	—
Vessel volume that includes the lumen and wall	0.0004	−0.0001	0.001	0.0003	1.641	0.105	8.702	2.541	14.863	3.091	2.815	0.006
Maximum cross-sectional calcified area	−0.173	−0.416	0.070	0.122	−1.420	0.160	—	—	—	—	—	—
Maximum cross-sectional dilation based on lumen diameter	−1.231	−2.317	−0.144	−0.549	−2.258	0.027	−1.351	−2.496	−0.206	0.574	−2.352	0.021
Maximum lipid-rich necrotic core area	0.431	0.099	0.763	0.166	2.589	0.012	23.45	4.421	42.47	9.548	2.456	0.016
Thickest wall across all cross sections of the target	4.713	1.523	7.904	1.600	2.946	0.004	8.344	1.107	15.582	3.632	2.298	0.024
Maximum cross-sectional wall area	0.155	0.065	0.245	0.045	3.435	0.001	0.128	0.052	0.204	0.038	3.372	0.001
Minimum cross-sectional lumen area	−0.452	−1.073	0.169	−0.311	−1.452	0.151	—	—	—	—	—	—
Wall volume divided by vessel volume inclusive of lumen and wall	7.110	0.225	13.994	3.452	2.060	0.043	7.737	−2.619	18.094	5.196	1.489	0.141

TABLE 4.

Differences Between the Observed ASCVD and the ASCVDs Predicted by Models 1 and 2

		95% Limits of Agreement	
	Bias	**Lower**	**Upper**
Observed ASCVD vs ASCVD predicted by model 1 (semiautomated approach, continuous imaging features)	−1.954 ± 10.88	−23.29	19.38
Observed ASCVD vs ASCVD predicted by model 2 (semiautomated approach, dichotomized imaging features)	−1.466 ± 12.04	−25.06	22.13
ASCVD predicted by model 1 vs ASCVD predicted by model 2	0.488 ± 5.88	−11.04	12.01

J Comput Assist Tomogr. Author manuscript; available in PMC 2021 April 28.